Eigenvalue equalization filtered-x (EE-FXLMS) algorithm applied to the active minimization of tractor noise in a mock cabin

Jared K. Thomas,[a] Stephan Lovstedt,[b] Jonathan D. Blotter,[c] Scott D. Sommerfeldt[d] and Ben Faber[e]

(Received 6 July 2007; revised 6 December 2007; accepted 7 December 2007)

The active control of tractor noise requires the ability to track and control a signal that changes in frequency as the speed of the engine, in revolutions per minute (rpm), changes during operation. The most common control approach is typically based on some version of the filtered-x algorithm. For this algorithm, the convergence and tracking speed are functions of the frequency dependent eigenvalues of the filtered-x autocorrelation matrix. To maintain stability, the system must be implemented based on the slowest converging frequency that will be encountered. This often leads to significant degradation in the overall performance of the control system. This paper will present an approach which largely overcomes this frequency dependent performance, maintains a relatively simple control implementation, and improves the overall performance of the control system. The control approach is called the eigenvalue equalization filtered-x least mean squares (EE-FXLMS) algorithm and its effectiveness will be demonstrated through an application to tractor noise in a mock cab. Experimental results will be presented which show that the EE-FXLMS algorithm has faster convergence times and provides on average a 1 dB increase in attenuation. A 3.5 dB increase in attenuation was seen in some of the cases presented.

Primary subject classification: 38.3; Secondary subject classification: 13.7

1 INTRODUCTION

The most common control approach for the active noise control (ANC) of stationary or time-varying frequencies is typically based on some version of the filtered-x least mean squares (FXLMS) algorithm[1,2]. Though the FXLMS algorithm has proven successful for many applications, one of its limitations is that it exhibits frequency dependent convergence and tracking behavior leading to a significant degradation in the overall performance of the control system. The performance degradation is especially evident for the case of non-stationary noise, such as tractor noise, where the target noise is likely to take on every frequency in the range where control is possible. In these cases, less attenuation is seen at the frequencies where the convergence of the algorithm is slow. Solutions to the frequency dependent problem have been proposed such as the HLMS algorithm by Clark and Gibbs[3], and similar work by Lee et al.[4], the FxGAL algorithm by Vicente and Masgrau[5], the work of Kuo et al.[6], the modified FXLMS algorithm[7], or the normalized FXLMS. The drawback of most of these approaches is that they either increase the computational burden of the algorithm, increase the algorithm's complexity, or are only effective for specific applications.

This paper will discuss a new approach that has been developed which largely overcomes this frequency dependent performance, and improves the overall performance. The approach is relatively simple to implement, can be added to existing FXLMS algorithms with only minor modifications, and does not increase the computational burden of the algorithm. The approach is valid for both single, and multiple input/output implementations. The effectiveness of the

[a] Department of Mechanical Engineering, 435 CTB, Brigham Young University, Provo UT 84602; email: jthomas@byu.edu
[b] Department of Physics and Astronomy, N283 ESC, Brigham Young University, Provo UT 84602; email: s_lovstedt@yahoo.com
[c] Department of Mechanical Engineering, 435 CTB, Brigham Young University, Provo UT 84602; email: jblotter@byu.edu
[d] Department of Physics and Astronomy, N283 ESC, Brigham Young University, Provo UT 84602; email: scott_sommerfeldt@byu.edu
[e] Faber Acoustical; email: ben@faberacoustical.com

approach will be demonstrated through an application to tractor noise in a mock cabin.

2 BACKGROUND

For this research, a feedforward implementation of the FXLMS algorithm is used which relies on a reference signal being "fed" forward to the control algorithm so that it can predict in advance the control signal needed to attenuate the unwanted noise. A feedforward implementation of the FXLMS algorithm involves adaptive signal processing to filter the reference signal in such a way that the measured residual noise is minimized. The measured residual is called the error signal and for this research it will be measured as an energy density (ED) quantity. The advantages of an ED based FXLMS algorithm[8] for noise in an enclosure[9,10] and for the application of tractor engine noise[11,12] are well documented. Before introducing the new control approach, a brief explanation of the general FXLMS algorithm is given. The extension of the general FXLMS algorithm to an ED based FXLMS is straightforward and well documented in Ref. 8.

2.1 FXLMS

The goal of the FXLMS algorithm is to reduce the mean-squared value of the error signal at a location where the sound is to be minimized. Boucher, Elliot, and Nelson[13] provide a good reference for the derivation of the single channel FXLMS algorithm, which is shown in block diagram form in Fig. 1. In the figure, and in all equations presented, the variable t is used as a discrete time index and the variable z is used as a discrete frequency domain index.

The mean-squared value of the error signal is a quadratic function (a "bowl") with a unique global minimum. For each iteration of the algorithm, $\mathbf{W}(z)$, an adaptive FIR control filter, takes a step of size μ, the convergence coefficient, times the gradient of the squared error signal in search of a single global minimum that represents the smallest attainable mean-squared value of the error signal. The control filter update equation for $\mathbf{w}$ can be expressed in vector notation as

$$\mathbf{w}(t+1) = \mathbf{w}(t) - \mu e(t)\mathbf{r}(t) \qquad (1)$$

where e(t) is the error signal and $\mathbf{r}(t)$ and $\mathbf{w}(t)$ are defined as

$$\mathbf{r}^T(t) = [r(t), r(t-1), \ldots, r(t-I+1)] \qquad (2)$$

$$\mathbf{w}^T(t) = [w_0, w_1, \ldots, w_{I-1}]. \qquad (3)$$

The filtered-x signal, r(t), is the convolution of $\hat{\mathbf{h}}(t)$, the estimate of the secondary path transfer function, and x(t), the reference signal. The secondary path transfer function is represented as an impulse response that includes the effects of digital-to-analog converters, reconstruction filters, audio power amplifiers, loudspeakers, the acoustical transmission path, error sensors, signal conditioning, anti-alias filters, and analog-to-digital converters. This secondary path transfer function has a large effect on the performance of the algorithm.

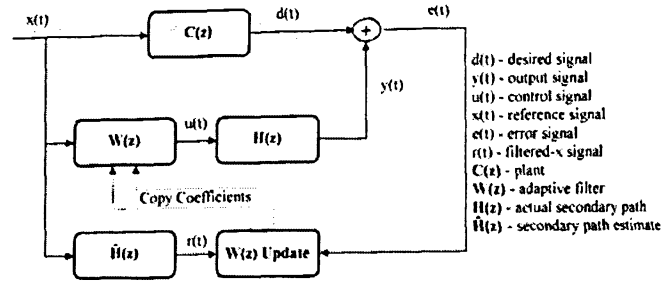

Fig. 1—Block diagram of the FXLMS Algorithm.

2.2 Secondary Path Transfer Function

One difficulty in implementing the FXLMS algorithm is that the secondary path, represented as $\mathbf{H}(z)$ in Fig. 1, is unknown. An estimate, $\hat{\mathbf{H}}(z)$, of the secondary path must be used. The estimate is obtained through a process called system identification (SysID).

The SysID process to obtain $\hat{\mathbf{H}}(z)$ is performed either online (while ANC is running), or offline (before ANC is started). For the fastest convergence of the algorithm, an offline approach is used. The offline SysID process is performed before ANC is started and consists of playing white noise through the control speaker and measuring the response at the error sensor. The measured transfer function is a finite impulse response (FIR) filter, $\hat{\mathbf{h}}(t)$, that represents $\hat{\mathbf{H}}(z)$. The coefficients of $\hat{\mathbf{h}}(t)$ are stored and used to run control.

3 FREQUENCY DEPENDENT CONVERGENCE BEHAVIOR

The inclusion of $\hat{\mathbf{H}}(z)$, while absolutely necessary for algorithm stability, degrades performance by slowing the algorithm's convergence. One reason for the decreased performance is the delay associated with $\hat{\mathbf{H}}(z)$. For many ANC applications, such as enclosures of less than a few meters, the delay is on the order of 10 ms or less and convergence is still rapid[14]. A more significant problem is that the inclusion of $\hat{\mathbf{H}}(z)$ causes frequency dependent convergence behavior. The frequency dependent behavior can be better understood by looking at the eigenvalues of the autocorrelation matrix of the filtered-x signal, which is largely a function of $\hat{\mathbf{H}}(z)$.

The eigenvalues of the autocorrelation matrix of the filtered-x signal relate to the dynamics or time constants of the modes of the system. Typically, a large spread is observed in the eigenvalues of this matrix, corresponding to fast and slow modes of convergence. For a given fixed value of the convergence parameter, μ, some of the modes converge faster than others. As the frequency of the reference signal changes, the optimal value of μ would also change, with larger values of μ being used for slower modes to help them converge more rapidly. The fastest modes have the fastest convergence and the greatest reduction potential, but limit how large of a convergence parameter, μ, can be used[15]. If μ is increased beyond this limit, the convergence at frequencies associated with slower modes will be faster, but the system will become unstable at frequencies associated with faster modes.

The autocorrelation matrix of the filtered-x signal is defined as

$$\mathbf{R} = E[\mathbf{r}(t)\mathbf{r}^T(t)] \tag{4}$$

where $E[\ ]$ denotes the expected value of the operand which is the filtered-x signal vector, $\mathbf{r}(t)$, multiplied by the filtered-x signal vector transposed, $\mathbf{r}^T(t)$. In general, it has been shown that the FXLMS algorithm (or any of its variations) will converge (in the mean) and remain stable as long as the chosen μ satisfies the following equation[16]

$$0 < \mu < \frac{2}{\lambda_{max}}. \tag{5}$$

In Eqn. (5), λ_{max} is the maximum eigenvalue of the autocorrelation matrix for the filtered-x signal in the range of frequencies targeted for control. The eigenvalues of $\mathbf{R}$ are associated with the characteristic equation

$$[\mathbf{R} - \lambda\mathbf{I}]\mathbf{Q}_n = 0 \tag{6}$$

where $\mathbf{I}$ is the identify matrix, $\mathbf{Q}_n$ is a column vector (eigenvector), and λ is a scalar variable (eigenvalue). The eigenvalues are found as the solutions of the equation

$$\det[\mathbf{R} - \lambda\mathbf{I}] = 0 \tag{7}$$

where det indicates the determinant of the matrix. Since the autocorrelation matrix, $\mathbf{R}$, is positive semidefinite, the eigenvalues are all real and non-negative. In practice, it is too computationally demanding to obtain a real-time estimate of the autocorrelation matrix so the optimal μ is often selected through experimentation. An offline estimate of the autocorrelation matrix is made by taking an actual $\hat{\mathbf{H}}(z)$ model from a mock cabin and importing it into a numerical computer package. If a single frequency reference signal is used, λ_{max} can be computed for that frequency. If the simulation is repeated over a range of frequencies, λ_{max} for each frequency can be found. Figure 2 shows an offline simulation using an actual $\hat{\mathbf{H}}(z)$ from a mock cab, and tonal inputs from 0–500 Hz. The eigenvalues in the figure have been normalized to the largest eigenvalue in the range.

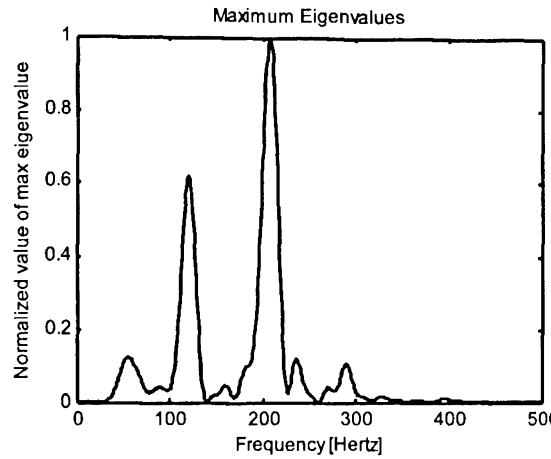

Fig. 2—Plot of normalized maximum eigenvalues of the autocorrelation matrix over frequency.

Figure 2 illustrates the frequency dependent behavior. The largest eigenvalue occurs at about 210 Hz. This location corresponds to the largest stable μ in the frequency range from 0–500 Hz as given by Eqn. (5). Most other frequencies have a smaller eigenvalue and could use a larger μ, and still be stable, if only that particular frequency was targeted for control. Frequencies at the valleys of the figure have the smallest eigenvalues and could use the largest μ's and still be stable, again if they were the only frequencies targeted for control. For dynamic signals, larger μ's are desirable as they lead to faster convergence and thus increased attenuation. Larger μ's also increase gradient search noise and thus increase the excess mean square error. This effect is insignificant compared to the benefit of improved tracking ability for dynamic signals.

If the frequency range for control is 0–500 Hz, the μ associated with 210 Hz (the smallest in the range) must be used for stability. If for example, 100 Hz was the only tone targeted for control a μ larger than the one used at 210 Hz could be used and convergence would be faster. If both 100 and 210 Hz were targeted for control, the smaller μ associated with 210 Hz must be used for stability and degraded performance at 100 Hz is expected. In summary, because the μ associated with the largest eigenvalue in the range of frequencies targeted for control must be used for stability, degraded performance is expected at the other frequencies in the range that would benefit from the use of a larger μ.

4 EIGENVALUE EQUALIZATION

If the variance in the eigenvalues of the autocorrelation matrix was minimized, a single convergence parameter could then be chosen that would converge at nearly the same rate over all frequencies. As previously stated, the autocorrelation matrix is directly dependent on the filtered-x signal, which is computed by filtering the input reference signal with $\hat{\mathbf{H}}(z)$. Often times it is either impossible or undesirable to alter the reference signal. Assuming the reference signal is left unchanged, changes to the autocorrelation matrix must stem from changes to $\hat{\mathbf{H}}(z)$, but must be done carefully as errors in its estimation already contribute to slower convergence rates and instability. Estimation errors can be considered in two parts: errors in the amplitude estimation and errors in the phase estimation[17]. It has been shown that phase estimation errors greater than ±90 degrees cause algorithm instability[13], but errors as high as 40 degrees have little effect on the performance[13]. Magnitude estimation errors can be compensated for by the choice of μ[16,18], and consequently do not affect stability. Ideally, changes would be made to the magnitude information of $\hat{\mathbf{H}}(z)$, while the phase information is preserved. Essentially an all-pass filter with the same phase characteristic as that of $\hat{H}(z)$ is designed.

The idea to remove the variance in the eigenvalues by changing the magnitude coefficients of $\hat{\mathbf{H}}(z)$, while preserving the phase will be referred to as the eigenvalue equalization filtered-x least mean squares (EE-FXLMS) algorithm approach. There are many ways that the magnitude coefficients could be adjusted. The remainder of this paper will focus on one method of adjusting the magnitude coefficients that is simple to implement, and offers significant improvement in the overall sound reduction.

The basic procedure for implementing the EE-FXLMS is to adjust the coefficients of $\hat{\mathbf{h}}(t)$ before ANC control is started as follows:

1. Get the time domain impulse response $\hat{\mathbf{h}}(t)$ for each $\hat{\mathbf{H}}(z)$ through an offline SysID process.
2. Take the Fast Fourier Transform (FFT) to obtain $\hat{\mathbf{H}}(z)$.
3. Divide each value in the FFT by its magnitude and then multiply by the mean value of the FFT.
4. Compute the inverse FFT to obtain a new $\hat{\mathbf{h}}(t)$ and use the new modified $\hat{\mathbf{h}}(t)$ in the FXLMS algorithm as normal.

This procedure flattens the magnitude coefficients of $\hat{\mathbf{H}}(z)$ while preserving the phase. If using multiple channel and/or ED control, the process is repeated for each $\hat{\mathbf{h}}(t)$ estimate. In general there will be one $\hat{\mathbf{h}}(t)$ for each channel for squared pressure control and three for each channel for ED control with a 2D error sensor as used in this paper (one for pressure, one for each of two velocity directions). It is an offline process done directly following SysID, and can be incorporated into any existing algorithm with only a few lines of code. As an offline process, it adds no computational burden to the algorithm when control is running. The results of the flattening process can be seen in Figs. 3 and 4. Figure 3 shows the original and modified $\hat{\mathbf{H}}(z)$ magnitude coefficients and Fig. 4 shows that the phase information of $\hat{\mathbf{H}}(z)$ has been preserved. Note in Fig. 4 that the two lines representing the original and modified phase information of $\hat{\mathbf{H}}(z)$ are directly on top of each other.

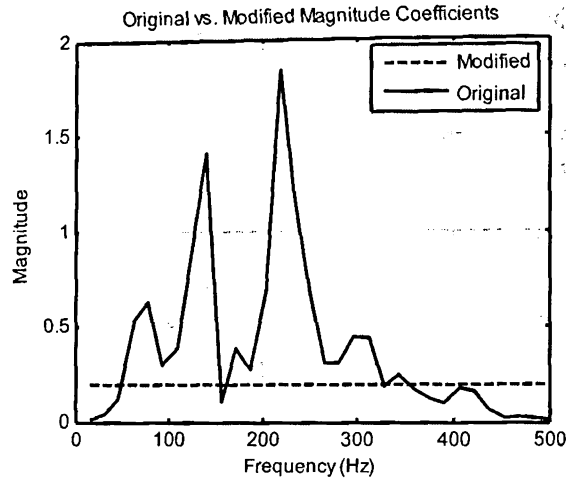

Fig. 3—Original and modified magnitude coefficients of $\hat{\mathbf{H}}(z)$.

An attempt to quantify any improvement in the eigenvalue spread has been made by using the following metrics:

1. *Span*—$(\lambda_{max}/\lambda_{min})$. Ideally one.

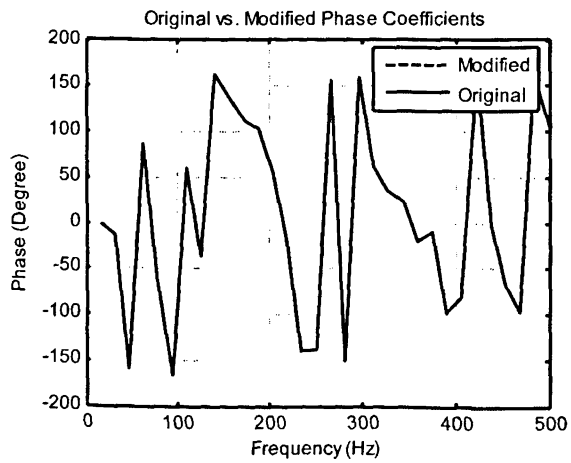

Fig. 4—Original and modified phase coefficients of $\hat{\mathbf{H}}(z)$.

$$\frac{\lambda_{max}}{\lambda_{min}} \tag{8}$$

2. *RMS value*—root mean square. Ideally one.

$$\sqrt{\langle \lambda^2 \rangle} \text{ (where } \langle \ldots \rangle \text{ denotes the arithmetic mean)} \tag{9}$$

3. *Crest factor*—λ_{max} divided by RMS value. (how close the RMS value is to the peak value) Ideally one.

$$\frac{\lambda_{max}}{\lambda_{rms}} \tag{10}$$

The effect of the flattening process on the eigenvalues can be seen in Fig. 5. The data for the figure were computed as before by an offline estimate of the autocorrelation matrix using an actual $\hat{\mathbf{H}}(z)$ model from a mock cabin and finding the λ_{max} for each frequency from 0–500 Hz. The curve labeled "Original" represents the same data shown in Fig. 2, and the curve labeled "Modified" is an estimate of the eigenvalues using the modified $\hat{\mathbf{H}}(z)$ model. In Fig. 5, the eigenvalues in both the original, and modified case, have been normalized by the largest of the original eigenvalues. It is seen that the modified eigenvalues are more uniform ("equalized") over all frequencies. The variation in the modified eigenvalues would be ideally zero. Because of finite frequency resolution the magnitude can only be constrained to be "flat" at frequency bin values. The variation in the eigenvalues is zero at those bins and the variation over all frequencies is greatly reduced, although some variation is still apparent between bin values. The decreased variation compared to the original eigenvalues should produce an observable performance advantage. The algorithm should converge at near the same rate over all frequencies, and should not exhibit the frequency dependent behavior of the standard FXLMS.

Table 1 shows the improvement of the modified eigenvalues according to the defined metrics. In Table 1, it can be seen that the modified case has a lower span, higher RMS value, and a lower crest factor. In all three metrics, the values for the modified case are closer to the optimum values that would be present if the eigenvalues across all frequencies were exactly the same. While possibly not the optimum, the modification to $\hat{\mathbf{H}}(z)$ that gives these improved eigenvalues makes a noticeable improvement in the performance of the algorithm.

5 EXPERIMENTAL RESULTS

The performance advantages of the EE-FXLMS control approach were verified for the case of a single frequency disturbance, a single time-varying frequency, and recorded tractor engine noise.

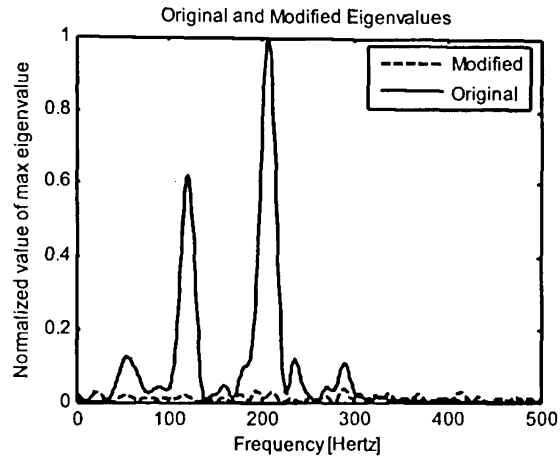

Fig. 5—Normalized original and modified eigenvalues.

5.1 Experimental Setup

The experiments were conducted inside a mock tractor cabin with nominal dimensions of 1.0 m × 1.5 m × 1.1 m. The cabin has a steel frame, 0.01 m thick plywood sides, and a 0.003 m thick Plexiglass® front panel. A speaker placed under a chair served as the sound source and three loudspeakers were setup in a two channel control configuration. The control signals were routed through a crossover circuit to route the low-frequency content (below 90 Hz) of both channels to a subwoofer on the floor of the cab, and to route the high-frequency content (above 90 Hz) of each control channel to one of two smaller satellite speakers mounted in the top corners of the cab, near the back. An ED error sensor consisting of four equally spaced microphones around a small disk was placed on the ceiling near where the operator's head would be. A photo of the cab, error sensor, and speakers is seen in Fig. 6.

The control algorithms were implemented on a Texas Instruments TMS320C6713 DSP processor. Both adaptive control filters consisted of 32 taps, and all secondary path transfer functions were modeled with 128 taps. All input channels were simultaneously sampled at 2 kHz, and all input and output signals had 16 bits of resolution. Fourth-order Butterworth lowpass

Table 1—Comparison of original and modified eigenvalues using defined metrics.

Metric	Original	Modified	% Improvement
Span	1.50e4	347	97.7
RMS	0.202	0.349	72.7
Crest Factor	4.94	2.87	41.9

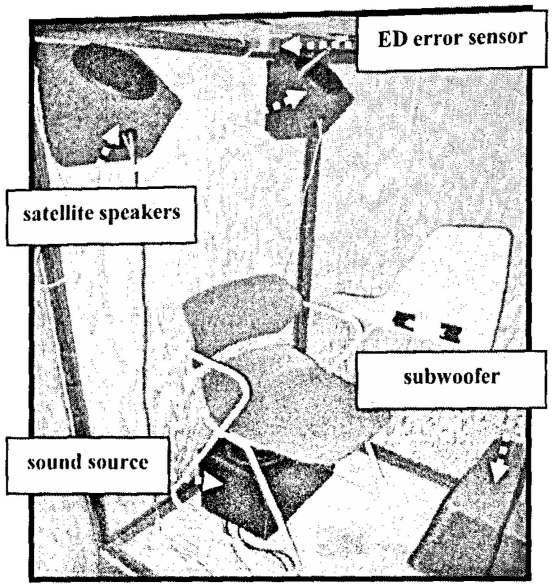

Fig. 6—Photo of inside of mock cab.

filters (400 Hz cutoff) provided anti-aliasing and reconstruction of input and output signals, respectively.

The controller performance was monitored in the cab using the ED error sensor, and eleven precision microphones. Ten of the microphones were equally spaced in two horizontal planes, located 0.15 m and 0.45 m from the cab ceiling. The eleventh microphone was placed where the operator's ear would be; about 0.30 m from the cab ceiling. Diagrams of the microphone locations can be seen in Fig. 7 (side view) and Fig. 8 (top view). The microphones were placed in several different measurement groupings to obtain estimates of how well the control was performing both locally (near the operator's head), and globally throughout the cabin. The measurement groupings can be seen in Fig. 8.

5.2 Single Frequency Disturbance

A function generator was used to generate single sinusoids at seven different frequencies (50 Hz, 80 Hz,

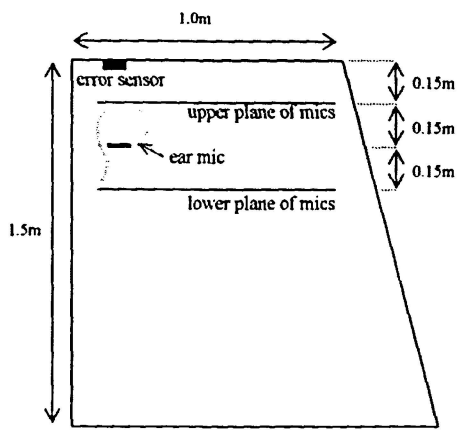

Fig. 7—Diagram of microphone locations in mock cab (side view).

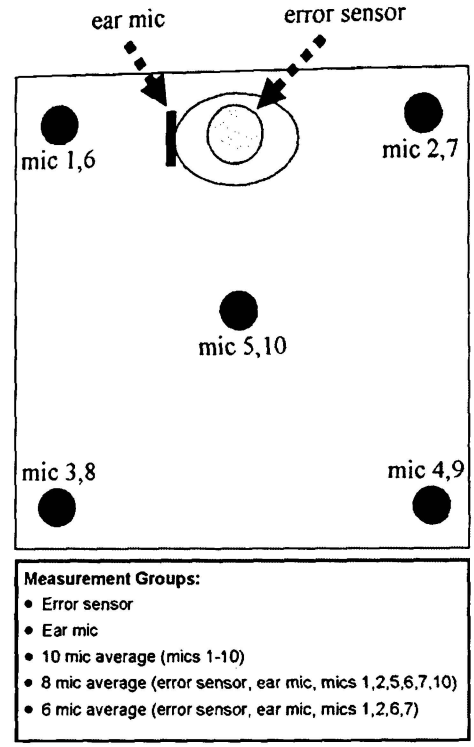

Fig. 8—Diagram of microphone locations in mock cab (top view) and measurement groupings.

113 Hz, 125 Hz, 154 Hz, 171 Hz, and 195 Hz). These frequencies correspond with the resonance frequencies of the cab (see Fig. 3). The convergence coefficient, μ, was determined experimentally for each frequency by finding the largest stable value and then scaling it back by a factor of ten to ensure stability. The measured performance for each configuration was the amount of attenuation in dB at the error sensor and the convergence time in seconds. The convergence time was taken to be a measure of how long it took the error signal, from the time that control was enabled to reach 1/e of its initial value (about 9 dB attenuation), where e is the base of the natural logarithm. The reason for choosing this was that the convergence time essentially becomes a measure of the rate of attenuation, which was felt to be useful when comparing cases where the overall level of attenuation may be significantly different. Each measurement was performed three times for computation of an average and to give a sense of the measurement's reproducibility. The results are shown in Table 2. In the table, EE refers to the EE-FLXMS implementation, and normal refers to the standard FXLMS implementation. The "reproducibility" shown in Table 2 was calculated in the same manner as a standard deviation, although it is recognized that the small sample size precludes referring to the result as a statistically valid standard deviation.

The results in Table 2 show that on average, over all of the frequencies tested, the EE-FXLMS converged

Table 2—Results of single frequency experimentation.

			Attenuation (dB)		Convergence Time (sec)	
Code Type	Freq. (Hz)	μ	Avg.	Reproducibility	Avg.	Reproducibility
Normal	50	1.E−08	37.85	0.34	0.26	0.02
EE	50	4.E−08	36.98	0.41	0.21	0.04
Normal	80	1.E−07	20.35	0.06	0.21	0.05
EE	80	2.E−07	21.77	0.02	0.30	0.02
Normal	113	1.E−08	13.69	0.01	0.44	0.04
EE	113	5.E−08	15.63	0.01	0.44	0.02
Normal	125	6.E−08	22.43	0.02	0.14	0.01
EE	125	7.E−07	23.68	0.01	0.11	0.01
Normal	154	3.E−08	1.91	0.01	5.00	0.01
EE	154	1.E−07	5.26	0.03	0.21	0.00
Normal	171	2.E−07	3.94	0.02	2.01	2.59
EE	171	9.E−07	6.61	0.01	0.36	0.16
Normal	195	9.E−08	16.43	0.29	0.49	0.12
EE	195	3.E−07	15.32	0.08	0.36	0.04
Total Average		Normal	16.66	0.08	1.22	0.40
		EE	17.89	0.11	0.27	0.04

about a second faster and had a little over 1 dB more attenuation at the error sensor. In addition, the variation for EE-FXLMS was smaller than the variation for the normal FXLMS. Table 2 also shows that the greatest decreases in convergence time occurred at 154 Hz and 171 Hz with a difference of several seconds being seen at these frequencies. 154 Hz and 171 Hz correspond to the two largest resonance modes of the cab below 200 Hz, and are places where the normal FXLMS exhibits slow convergence.

The advantage of the EE-FXLMS having a faster, more uniform convergence will be shown for the case of time-varying frequencies in the form of increased attenuation as the algorithm can more quickly converge on each frequency before the frequency shifts and the algorithm must reconverge.

5.3 Single Time-Varying Frequency

Several swept sine test signals with different sweep rates were created. Each test signal consisted of a swept sine from 50–200 Hz and the rates ranged from 2 Hz/sec to 265 Hz/sec. The time-averaged sound pressure level over the entire duration of the test signal was measured with and without control running. The convergence coefficient, μ, was determined experimentally by finding the largest stable value for the entire frequency range and then scaling it back by a factor of ten to ensure stability. The μ for EE-FXLMS control was found to be 1e-7 and the μ for standard FXLMS control was found to be 1e-8. The attenuation in dB was recorded at the measurement locations shown in Fig. 8. Each measurement was performed three times for computation of an average and to give a sense of the measurement reproducibility. The actual attenuation for both control types is shown in Table 3. The difference in attenuation between EE-FXLMS and FXLMS control is shown in Table 4. A positive number indicates EE-FXLMS performed better. The variation for each test case was small (usually less that 0.02 dB) and is not reported in either table.

The data show that averaged over all of the data, EE-FXLMS performs 1.0 dB better than normal FXLMS at the error sensor and about 0.8 dB globally. The data also show that the slower the sweep rate the more advantage EE-FXLMS provides. For the 2 Hz/sec sweep rate, EE-FXLMS control provides 2–3.5 dB more reduction. At the fastest sweep rates, the differences were almost negligible. It is postulated that for very fast sweep rates the signal changes so rapidly that the improved tracking ability of the EE-FXLMS is obscured, since the frequency is changing more rapidly than the algorithm is capable of converging. On the other hand, for slower sweep rates, the algorithm has sufficient time to converge and track the changing frequency.

5.4 Tractor Engine Noise

The performance advantages of EE-FXLMS were tested for the application of tractor noise. Tractor recordings were obtained for a CAT wheel-loader tractor for different operating conditions. As part of the recordings, the engine tachometer signal was recorded to use as the reference signal. The recordings were played through the source speaker, and measurements

Table 3—Results of time-varying frequency experimentation for EE-FXLMS and normal FXLMS control.

Sweep Rate	Control Type	Ear Mic Avg. (dB)	Error Mic Avg. (dB)	10 Mic Avg. (dB)	8 Mic Avg. (dB)	5 Mic Avg. (dB)
2 Hz/sec	Normal	4.92	6.45	3.62	4.82	5.28
	EE	7.78	10.01	5.88	7.79	8.52
4 Hz/sec	Normal	3.80	5.18	2.60	3.69	4.12
	EE	5.12	7.34	3.37	5.09	5.76
8 Hz/sec	Normal	3.25	4.27	2.13	3.05	3.43
	EE	3.97	5.72	2.49	3.86	4.41
16 Hz/sec	Normal	3.23	4.42	2.03	3.03	3.45
	EE	3.87	5.48	2.47	3.75	4.28
32 Hz/sec	Normal	2.87	3.99	1.71	2.66	3.07
	EE	3.02	4.32	1.79	2.85	3.31
64 Hz/sec	Normal	2.76	3.87	1.61	2.54	2.95
	EE	2.91	4.09	1.80	2.74	3.16
128 Hz/sec	Normal	2.71	3.85	1.54	2.49	2.90
	EE	2.63	3.90	1.47	2.45	2.89
256 Hz/sec	Normal	2.71	3.88	1.55	2.50	2.91
	EE	2.61	3.87	1.47	2.44	2.87

were taken in the same manner as the single time varying frequency measurements for both the EE-FXLMS and normal FXLMS. The actual attenuation for slow, medium, and fast sweep rates of the engine rpm is shown in Table 5. The difference in attenuation between EE-FXLMS and FXLMS is shown in Table 6. A positive number indicates EE-FXLMS performed better. The variation for each test case was small (usually less than 0.02 dB) and is not reported in either table.

Similar performance advantages for the EE-FXLMS were seen with the tractor recording experiments. On average EE-FXLMS performed 0.9 dB better at the error sensor and globally 0.85 dB better than the normal case.

6 CONCLUSIONS

A new eigenvalue equalization approach (EE-FXLMS) has been demonstrated for the case of engine noise in a mock cabin. It has been shown that adjustments to the magnitude coefficients of $\hat{\mathbf{H}}(z)$, while preserving the phase, leads to a more uniform eigenvalue spread, faster convergence times, and

Table 4—Comparison of EE-FXLMS and normal FXLMS control for time-varying frequency experimentation. A positive number indicates that EE-FXLMS control performed better.

Sweep Rate	Ear Mic Avg. (dB)	Error Mic Avg. (dB)	10 Mic Avg. (dB)	8 Mic Avg. (dB)	5 Mic Avg. (dB)
2 Hz/sec	2.86	3.56	2.26	2.97	3.24
4 Hz/sec	1.33	2.16	0.77	1.40	1.64
8 Hz/sec	0.72	1.45	0.35	0.80	0.98
16 Hz/sec	0.64	1.06	0.44	0.72	0.83
32 Hz/sec	0.14	0.33	0.08	0.19	0.24
64 Hz/sec	0.15	0.22	0.19	0.20	0.21
128 Hz/sec	−0.07	0.06	−0.08	−0.04	−0.01
256 Hz/sec	−0.10	−0.01	−0.08	−0.06	−0.04

Total Average (dB)

	Ear Mic Avg.	Error Mic Avg.	10 Mic Avg.	8 Mic Avg.	5 Mic Avg.	Total Avg.
Average	0.71	1.10	0.49	0.77	0.89	0.79

Table 5—Results of tractor engine noise experimentation for EE-FXLMS and normal FXLMS control. Slow, medium, and fast ramp refers to how fast the rpm of the tractor engine was increased (ramped up) during testing.

Sweep Rate	Control Type	Ear Mic Avg. (dB)	Error Mic Avg. (dB)	10 Mic Avg. (dB)	8 Mic Avg. (dB)	5 Mic Avg. (dB)
Slow ramp	Normal	4.05	4.60	3.46	3.95	4.10
	EE	5.03	5.58	4.31	4.90	5.07
Medium Ramp	Normal	2.22	2.47	1.88	2.14	2.23
	EE	3.45	3.82	2.95	3.35	3.48
Fast Ramp	Normal	0.48	0.48	0.41	0.48	0.50
	EE	0.88	0.83	0.80	0.88	0.91

Table 6—Comparison of EE-FXLMS and normal FXLMS control for tractor engine noise experimentation. A positive number indicates that EE-FXLMS control performed better. Slow, medium, and fast ramp refers to how fast the rpm of the tractor engine was increased (ramped up) during testing.

Sweep Rate	Ear Mic Avg. (dB)	Error Mic Avg. (dB)	10 Mic Avg. (dB)	8 Mic Avg. (dB)	5 Mic Avg. (dB)
Slow ramp	0.98	0.98	0.86	0.95	0.97
Medium Ramp	1.23	1.35	1.07	1.21	1.25
Fast Ramp	0.40	0.35	0.38	0.40	0.41
			Total Averages (dB)		
	Ear Mic Avg.	Error Mic Avg.	10 Mic Avg.	8 Mic Avg.	5 Mic Avg.	Total Avg.
Average	0.87	0.89	0.77	0.85	0.87	0.85

increased attenuation. The method of flattening the magnitude coefficients as part of the EE-FXLMS led to as much as 3.5 dB additional attentuation at the error sensor and 2.0–3.0 dB globally for the slower sweep rates. An additional attenuation of 1.0 dB at the error sensor and 0.5–1.0 dB globally was seen at sweep rates up to 16 Hz/sec, with a slight increase being seen at rates as high as 64 Hz/sec. Averaged over all of the sweep rates tested, EE-FXLMS provided 1 dB additional attenuation at the error sensor and 0.8 dB globally. For the tractor noise, on average EE-FXLMS performed 0.9 dB better at the error sensor and globally 0.85 dB better than the normal case.

The performance advantages of the EE-FXLMS become more meaningful when considering the simplicity of its implementation. It can be incorporated into any FXLMS algorithm with only a few lines of code. As an offline process, it does not increase the computational burden of the algorithm.

Flattening the magnitude coefficients is but one of many possible methods for adjusting the magnitude coefficients to improve the performance of FXLMS based algorithms. Future work will focus on an optimization approach to finding the values of the magnitude coefficients that lead to the best performance.

7 REFERENCES

1. D. R. Morgan, "An analysis of multiple correlation cancellation loops with a filter in the auxiliary path," *IEEE Trans. Acoust., Speech, Signal Process.* **28**, 454–467, (1980).
2. J. C. Burgess, "Active adaptive sound control in a duct: a computer simulation," *J. Acoust. Soc. Am.* **70**, 715–726, (1981).
3. R. L. Clark and G. P. Gibbs, "A novel approach to feedforward higher-harmonic control," *J. Acoust. Soc. Am.* **96**, 926–936, (1994).
4. S. M. Lee, H. J. Lee, C. H. Yoo, D. H. Youn and II W. Cha, "An active noise control algorithm for controlling multiple sinusoids," *J. Acoust. Soc. Am.* **104**, 248–254, (1998).
5. L. Vicente and E. Masgrau, "Fast convergence algorithms for active noise control in vehicles," *Proc. of Joint ASA/EAA/DEGA Meeting*, Berlin (1999).
6. S. M. Kuo, X. Kong, S. Chen and W. Hao, "Analysis and design of narrowband active noise control systems," *IEEE Trans. Acoust., Speech, Signal Process.* **6**, 3557–3560, (1980).
7. M. Rupp and A. H. Sayed, "Modified FXLMS algorithms with improved convergence performance," *IEEE Proc. of ASILOMAR-29* (1995).
8. S. D. Sommerfeldt and P. J. Nashif, "An adaptive filtered-x algorithm for energy-based active control," *J. Acoust. Soc. Am.* **96**, 300–306, (1994).

9. Y. C. Park and S. D. Sommerfeldt, "Global attenuation of broadband noise fields using energy density control," *J. Acoust. Soc. Am.* **101**, 350–359, (1997).
10. J. W. Parkins, S. D. Sommerfeldt and J. Tichy, "Narrowband and broadband active noise control in an enclosure using acoustic energy density," *J. Acoust. Soc. Am.* **108**, 192–203, (2000).
11. B. Faber and S. D. Sommerfeldt, "Global control in a mock tractor cabin using energy density," *Proc. ACTIVE '04*, Edited by Randolph H. Cabell and George C. Maling, Jr. (1994).
12. D. C. Copley, B. Faber and S. D. Sommerfeldt, "Energy density active noise control in an earthmoving machine cab," *Proc. NOISE-CON '05*, Edited by J. Stuart Bolton, Patricia Davies, and George C. Maling, Jr. (1995).
13. C. C. Boucher, S. J. Elliot and P. A. Nelson, "Effects of errors in the plant model on the performance of algorithms for adaptive feedforward control," *IEEE Proceedings-F* 138(4), 313–319, (1991).
14. S. J. Elliott and P. A. Nelson, "Active Noise Control," *IEEE Signal Process. Mag.* **10**, 12–35, (1993).
15. L. A. Sievers and A. H. von Flotow, "Comparison and extensions of control methods for narrow-band disturbance rejection," *IEEE Trans. Signal Process.* 40(10) (1992).
16. S. M. Kuo and D. R. Morgan, *Active Noise Control Systems, Algorithms and DSP Implementations*, Wiley-Interscience, 28, (1996).
17. S. D. Snyder and C. H. Hansen, "The effect of transfer function estimation errors of the filtered-x LMS algorithm," *IEEE Trans. Signal Process.* **42**(4), 950–953, (1994).
18. S. D. Snyder and C. H. Hansen, "The influence of transducer transfer functions and acoustic time delays on the implementations of the LMS algorithm in active noise control systems," *J. Sound Vib.* **141**(3), 409–424, (1990).